

MODELING and SIMULATION of ELECTROPATING PROCESS

Dr.Tahseen A.Al-Hattab
University of Babylon
Prof

Dr.Haydar A.Hussain
University of Babylon
Ass. Prof

Kadhim K. Kahlol
Institute of Kufa
Ass.Lecturer

ABSTRACT :-

In this study, it is acquainted with the kinetics of the chemical and electrochemical reactions by modeling and understanding of the essential and secondary (conjugate) chemical and electrochemical reactions during plating process . In addition , the effects of various conditions on the speed and kinetic of those reactions is also considered . In order to apply this manner , the mean-field kinetic equations and Poisson equation for charged lattice model are adopted using two types of one-dimensional cells for theoretical part of this study , namely (half and full cell) of size (100) with an applied potential of $(2KT/e)$. Provided that the cell should contain two identical electrodes of thickness (10) .A computer program in visual basic is specially constructed to show the results of this study as it should be . Through this program the concentrations are determined including (metallic atoms, cations, anions, solvents, vacancies and electrons) , the charges distribution and electrical potential across the sites. the results , during the three periods $(t = (1,3,5) \times 10^5)$, showed that under potential application across the cell , the deposition continues for long time then it is suppressed when the anode reaches failure limit , and it is observed that the deposition increases with the extension of space charges at the cathode , from the other hand , the ionic evolution (cation) will take a peak shape at the cathode , then it has a certain gradient between anode and cathode. A reversed situation occurs for the anions evolution . At the same time, electric potential distribution across the sites becomes higher resulting in deposition increasing .

نمذجة و محاكاة عمليات الطلاء الكهروكيميائي

الخلاصة :-

في هذه الدراسة تم التطرق الى معرفة حركيات التفاعلات الكيميائية و الكهروكيميائية من خلال فهم ونمذجة التفاعلات الكهروكيميائية الاساسية و التفاعلات الكيميائية المرافقة لها اثناء عملية الطلاء الكهروكيميائي وتأثير الظروف المختلفه على حركية وسرعة التفاعلات . تم الاعتماد على معادلات متوسط المجال الحركي ومعادلة بوزون المستعمله لنموذج شبكي مشحون ، وباستعمال نوعين من الخلايا باتجاه واحد لاغراض الجانب النظري في هذه الدراسة وهما (نصف الخلية ، والخلية الكاملة) ذات الحجم (100) تحت تأثير جهد مسلط مقداره $(2KT/e)$. حيث أن الخلية تحتوي على قطبين متماثلين سمك كل واحد منهما (10) . تم بناء برنامج حاسوبي بلغة فيجوال بيسك لحساب التراكيز وهي (الذرات المعدنية ، الايونات الموجبه ، الايونات السالبة ،

المذيب ، الفراغات ، الالكترونات) ، توزيع الشحنات والجهد الكهربائي عبر المواقع . فقد استعملت طريقة التدرج بالجهد الكيمياوي لحساب تيار الانتشار ، التي تعتمد عليها معادلات متوسط المجال الحركي . اظهرت النتائج خلال الفترات الزمنية الثلاثة ($t = (1,3,5) \times 10^5$) ، في حالة تسليط جهد عبر الخلية فأن الترسيب يزداد لفترات زمنية طويلة جدا ومن ثم يتوقف عند انهيار قطب الأنود ، ومن الملاحظ ان الترسيب يزداد عندما تزداد مساحة توزيع الشحنات عند قطب الكاثود هذا من جهة ، ومن جهة اخرى فأن النمو الايوني الموجب يكون على شكل قمة عند قطب الكاثود ويكون متدرج بين قطبي الانود والكاثود ، ويحصل العكس بالنسبة للنمو الايوني السالب ، وفي الوقت نفسه فأن توزيع الجهد الكهربائي عبر المواقع عندما يكون عالي يؤدي بالنتيجة الى زيادة الترسيب .

Keywords: electroplating; electrochemical reactions; dendritic growth; diffusion; lattice model.

1.INTRODUCTION :-

Electrochemical phenomena are ubiquitous in nature as well as in industry . Application includes for example batteries, fuel cells, catalysis processes , aluminum or magnesium electrolytic production, corrosion problems , electrodeposition and electroplating [Vincent,1997].

The important aspect of electrochemical process are dendritic growth (densely branches, shapes and branch thickness) , electrochemical reactions that happen inside the cell represented by oxidation-reduction processes at surface of anode and cathode , lattice model and mean-field kinetic equations (to calculate local concentrations inside the cell to simulate growth and dissolution) [Bernard,2001].

Barton and Bockris , showed the Barton and Bockris model of propagation , this model described growth in well- supported electrolytes , calling into question its applicability to polymer electrolyte systems . In addition ,the model assumed that propagation dendrite tips were relatively isolated and hemispherical in shape . Diggle et . al , improved the Barton and Bockris model of propagation [Barton ,1962][Diggle ,1969].

Mullins and Sekerka , developed linear stability analyses and stability criteria in one-dimensional thermal systems where surface tension forces slow the rate of solid deposition from melts. The Mullins-Sekerka method was extended to unsteady galvanostatic deposition from a two-dimensional semi-infinite region by Aogaki and Makino [Mullins ,1963][Aogaki ,1981].

Chen and Jorne , developed the most applicable fractal propagation model . Chazalviel , described migration-limited mechanisms in his work . Both approaches rely on the assumption that high voltages(10v) are applied to the electrochemical cell [Chen,1990][Chazalviel,1990].

Dobretsov et. al , studied spinodal decomposition in alloys where ordering and phase separation occur simultaneously. Chen , studied spinodal decomposition in a ternary system [Dobretsov,1996][Chen,1994].

Jean-Francois Gouyet and Mathis Plapp , used Cahn-Hilliard equations to perform numerical simulations in two dimensions of the growth of regular "snowflakes." It naturally showed curvature and kinetic effects at the interface as assumed by the classic phenomenological equations of dendritic growth. In addition, they found solute trapping. The dendrite tips were stabilized by the Gibbs- Thomson

boundary condition. They compare their models and the phase-field models and discuss the influence of noise [Jean,1996].

Mathis Plapp and Jean-François Gouyet , developed the mean-field kinetic equations for a lattice gas model of a binary alloy with vacancies (ABv model) in which diffusion takes place by a vacancy mechanism. These equations are applied to the study of phase separation of finite portions of an unstable mixture immersed in a stable vapor. Due to a larger mobility of surface atoms, the most unstable modes of spinodal decomposition are localized at the vapor-mixture interface. Simulations show checkerboard-like structures at the surface or surface-directed spinodal waves [Mathis,1999].

Bernard et. al, have built electrochemical mean-field kinetic equations modeling electrochemical cells and growth structures that form during electrodeposition. They confirmed the viability of this approach by simulating the ion kinetics in front of planar electrodes during growth on the cathode and dissolution of the anode(double layer, space charge, due to an anion depletion ahead of the growing front,...).Two dimensional simulations of growing dendrites are also presented [Bernard,2001].

Gouyet et. al, reviewed several methods to obtain mean-field kinetic equations, and discuss applications to the dynamics of order–disorder transitions, spinodal decomposition, and dendritic growth in the isothermal or chemical model. In the case of dendritic growth they showed that the mean field kinetic equations are equivalent to standard continuum equations and derive expressions for macroscopic quantities. In spinodal decomposition, they focused their attention on the vacancy, which is a more faithful picture of diffusion in solids than the more widely examined exchange mechanism. They have studied the interfaces between an unstable mixture and a stable ‘vapors’ phase, and analyze surface modes that lead to specific surface patterns [Gouyet,2003] .

Charles Monroe and John Newman , used two methods,Mullins-Sekerka linear stability analysis and the Barton and Bockris dendrite-propagation model . Both described cathodic roughening and dendritic growth and contain the effects of surface tension and local concentration deviations induced by surface roughening. Here, a kinetic model is developed which additionally includes mechanical forces such as elasticity, viscous drag, and pressure, showing their effect on exchange current densities and potentials at roughening interfaces[Charles,2004].

Paolini et. al , studied the kinetics of a system composed of charged particles may be described by an approximate method where a corresponding mean electric field created by the particles is used in place of the actual binary interaction. Results for the effective Coulomb interaction are illustrated by the deviation angle in deuteron-deuteron collision for some characteristic conditions found in Inertial Electrostatic Confinement devices (IEC). This equipment is used to confine high energy ions, such as deuteron and triton, in order to produce fusion reaction. Now is underway a study to use the effective interaction together with the Boltzmann Equation to describe the time evolution of the energy and angular momentum distribution of ions in an IEC device[Paolini,2009].

Candacek et. al , studied the structural transformations of siliconnano wires when cycled against lithium were evaluated using electrochemical potential spectroscopy and galvanostatic cycling. During the charge, the nanowires alloy with lithium to form an amorphous (Li , Si) compound .In studies on micron-sized particles previously reported in the literature, this transformation is a crystallization to a meta stable Li₁₅Si₄ phase[Candacek , 2009] .

2.THEORETICAL ANALYSIS :-

2.1. Lattice Gas Model :-

Lattice gas model is used to study and analyze the electrochemical process as a model involves various electrochemical mechanisms governing the dendritic growth and including charged particles and using simple microscopic characteristics to simulate the salient features of the electrochemical process consisting of both the diffusion kinetics of the charged and neutral species, and the oxido-reduction phenomena on the electrode interfaces. Due to non-availability of theoretical studies of the behavior of an entire electrochemical cell based on a microscopic model, lattice gas model are still used up to now to simulate the phenomena located on the electrode surfaces , such as adsorption or under potential deposition and for studies of ionic transport at liquid-liquid interfaces[Bernard ,2001].

In a two-dimensional lattice gas on a square lattice with lattice spacing (a) in figure(1) which shows this model , a fixed potential difference is applied across the cell. The ions in the electrolyte are subjected to an electric field E_k (and hence a force $F_k = qE_k$) at their lattice site position k . The various species have short-range interactions (here, attractive interactions are considered between solvent and ions, solvent and solvent, and metal and metal). Electron transfer takes place on the electrode surfaces . Cations M^+ give metallic atoms M^0 after reduction , while anions A^- are supposed to be nonelectroactive. Solvent S is neutral, but can interact through short-range interactions with other species and with itself. A microscopic configuration is specified by the set $\{n\}$ of the occupation numbers n_k^α on each site k : $n_k^\alpha = 1$ if k is occupied by species $\alpha = M^0, M^+, A^-, S$, or a vacancy v , and 0 otherwise. It is supposed that there is a steric exclusion between the different species, that is , a given site can be occupied by only one species or it can be empty (vacancy) [Bernard ,2002] :

$$\sum_{\alpha} n_k^{\alpha} + n_k^v = 1 \quad \rightarrow |a| \leftarrow \quad (1)$$

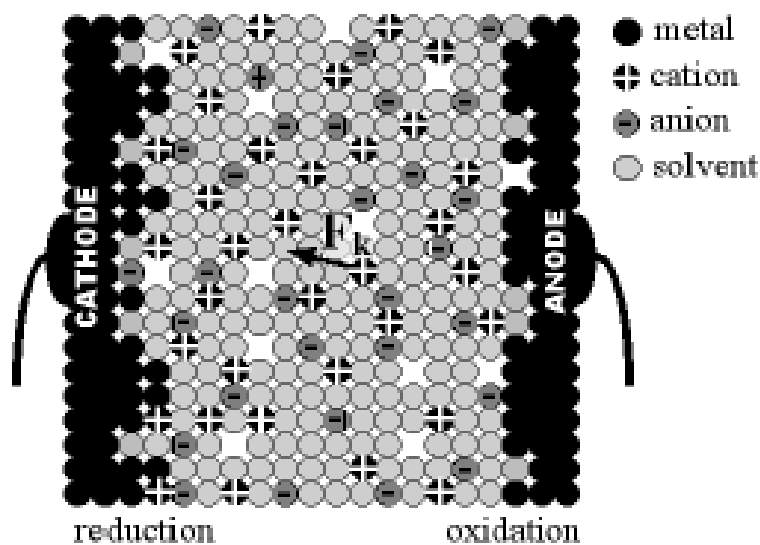


Fig. 1. The lattice-gas model considered in the present study[Bernard ,2001]

Two very different types of interactions are existed in the electrochemical cell depending on electric field intensity between charged species and the spacing among them , namely[Marc,2003]:-

1. Short-rang interactions: - Which are taking place between the nearest - neighbors and different - in - charge species having rather weak inter-connection bonds between different species such as (Van Der Waals forces , solvation effects , and chemical interactions).

2. Long-range interactions:- Occur between the species of higher intensities of electric fields separated by longer spaces having stronger inter - connection than the former type bonds such as (coulomb interactions between the charged species).In short-range interactions, the particle (metal, ion, or solvent) jumps to one of its vacant nearest-neighbor sites.

Also for charged particles, it depends on the local electric field that shifts the barrier height as shown i.e. for a moving particle carrying a charge (q) to be shifted from site k to site $k+a$ a long the jump path X , in the presence of electrical field , the potential energy is superimposed to the local potential of that particle as shown in figure (2) [Marc,2003] .

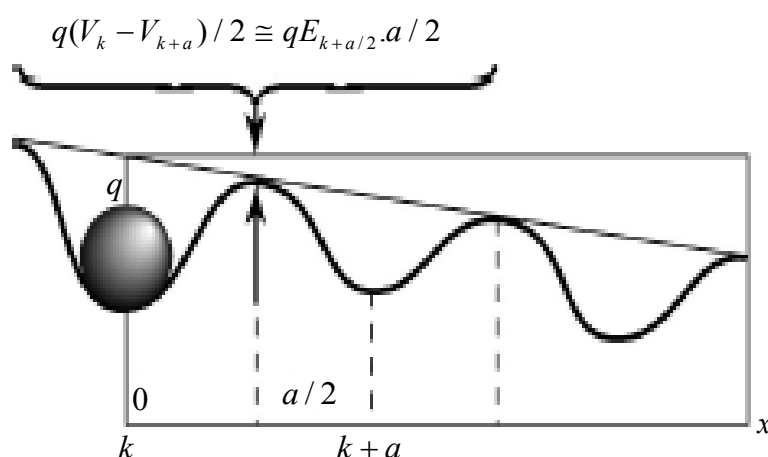


Fig.2. In the presence of electric field E , a potential energy, which varies, to first order, like $qE \cdot X$ along the jump path X , is superimposed to the local potential seen by a moving particle (with charge q) .

where:-

E : The electrical field , q : Charge of particle , X : The jump path

V_k : Electrical potential defined on the lattice sites k .

The result for the jump rate from site k to site $k+a$ is[Marc,2003] ,

$$\tilde{w}_{k,k+a}^{\alpha}(\{n\}) = w^{\alpha} \exp\left(\frac{1}{KT} \sum_{\beta} \sum_{a'} \varepsilon^{\alpha\beta} n_{k+a'}^{\beta}\right) \times \exp\left(\frac{q^{\alpha}}{2KT} (V_k - V_{k+a})\right) \quad (2)$$

where:- $\varepsilon^{\alpha\beta}$: The nearest - neighbor interactions between species α and β

KT : The (fixed) thermal energy , q^α : Charge for each species
 w^α : A fixed jump frequency that may be different for each species

2.2. Mean-Field Kinetic Equations

In the absence of electrochemical processes at the electrodes , the number of each type of particles remains constant, and the kinetic equation of the average concentration has the structure of a conservation equation

$$\frac{\partial P_k^\alpha}{\partial t} = - \sum_a \tilde{J}_{k,k+a}^\alpha \quad (3)$$

where:-

P_k^α : The concentration of species α at site k, a : spacing between neighbors species α .

$\tilde{J}_{k,k+a}^\alpha$: The diffusion current of species α on the bond linking site k to nearest neighbor site k+a.

The diffusion current of species α on the bond linking site k to nearest neighbor site k+a defined by two methods[Marc,2003] :-

a. First method:-

$$\begin{aligned} \tilde{J}_{k,k+a}^\alpha = w^\alpha [& P_k^\alpha P_{k+a}^\nu \exp(-\frac{1}{KT} \sum_\beta \sum_{a'} \varepsilon^{\alpha\beta} P_{k+a'}^\beta + \frac{q^\alpha}{2KT} (V_k - V_{k+a})) \\ & - P_{k+a}^\alpha P_k^\nu \times \exp(-\frac{1}{KT} \sum_\beta \sum_{a'} \varepsilon^{\alpha\beta} P_{k+a+a'}^\beta + \frac{q^\alpha}{2KT} (V_{k+a} - V_k))] \end{aligned} \quad (4)$$

b. Second method:-

$$\tilde{J}_{k,k+a}^\alpha = -\tilde{M}_{k,k+a}^\alpha D_a \tilde{\mu}_k^\alpha \quad (5)$$

In this method as the product of an electrochemical bond mobility \tilde{M}_{ij}^α a times the (discrete) gradient of an electrochemical potential $\tilde{\mu}_i^\alpha$.

Where D_a is a difference operator acting on the site coordinates, $D_a F_k = F_{k+a} - F_k$.

The electrochemical potential :

$$\tilde{\mu}_k^\alpha = \mu_k^\alpha + q^\alpha V_k = - \sum_\beta \sum_a \varepsilon^{\alpha\beta} p_{k+a}^\beta + KT \ln\left(\frac{p_k^\alpha}{p_k^\nu}\right) + q^\alpha V_k \quad (6)$$

where:-

$(-\sum_\beta \sum_a \varepsilon^{\alpha\beta} p_{k+a}^\beta)$: A local energy due to the interaction of species α with its local environment

$KT \ln\left(\frac{p_k^\alpha}{p_k^\nu}\right)$: An entropy term , $q^\alpha V_k$: electrostatic energy

The mobility along a bond k , k+a is given by:

$$\tilde{M}_{k,k+a}^\alpha = \frac{w^\alpha}{KT} P_k^\nu P_{k+a}^\nu \exp\left(\frac{(\tilde{\mu}_k^\alpha + \tilde{\mu}_{k+a}^\alpha)}{2KT}\right) shc \frac{D_a \tilde{\mu}_k^\alpha}{2KT} \quad (7)$$

where it is used the notation $\text{shc } u = \sinh u/u$ (close to equilibrium , $\tilde{\mu}_{k+a}^\alpha \cong \tilde{\mu}_k^\alpha$ and $\text{shc}[D_a \tilde{\mu}_k^\alpha / 2KT] \cong 1$).

2.3. The Poisson Equation

To determine the electrostatic potential for a given charge distribution, a discrete version of the Poisson equation is solved using the lowest order discretization for the Laplacian that involves only nearest neighbor sites[Bernard,2001] ,

$$\sum V_{k+a} - 4V_k = -\frac{a^{2-d}}{\epsilon} \sum_{\alpha=+,-,e} q^\alpha p_k^\alpha \tag{8}$$

where:-

q^α : The charge of species α ($q^e = -e$, for the electron).

a : The lattice spacing , d : the spatial dimension

$$\frac{\partial P_k^e}{\partial t} = -\sum_a \tilde{J}_{k,k+a}^e \tag{9}$$

where:-

$\tilde{J}_{k,k+a}^e$: Electronic current

The electronic current is then written as an electronic mobility times the discrete gradient of the chemical potential [Bernard,2002] ,

$$\tilde{J}_{k,k+a}^e = -\tilde{M}_{k,k+a}^e D_a \tilde{\mu}_k^e \tag{10}$$

where:-

$\tilde{M}_{k,k+a}^e$: Electronic mobility from k to $k+a$

$\tilde{\mu}_k^e$: The local chemical potential of the electron

The electronic mobility can be determined as[Marc,2003] ,

$$\tilde{M}_{k,k+a}^e = \frac{w^e}{KT} f(P_k^o) f(P_{k+a}^o) \tag{11}$$

where w^e is a constant frequency prefactor and f is an interpolation function that is equal to 1 for large metal concentrations and falls to zero for low metal concentrations. With this choice, the electronic jump probability is important only if nearest-neighbor sites k and $k+a$ have a large enough probability to be occupied by metallic atoms. It is used for f [Bernard,2002] .

$$f(P) = \frac{\tanh[(P - P_c)/\xi] + \tanh[P_c/\xi]}{\tanh[(1 - P_c)/\xi] + \tanh[P_c/\xi]} \tag{12}$$

a monotonic function that varies from 0 when $p = 0$ to 1 for $p = 1$, with a rapid increase through an interval in p of order ξ centered around some concentration P_c that is reminiscent of a percolation threshold. This interpolation is motivated by the fact that the metallic region must be dense enough to be connected in order to allow the electrons to propagate.

The local chemical potential of the electron is defined by [Bernard,2002] [Marc,2003] ,

$$\tilde{\mu}_k^e = E_f + q^e V_k + \frac{P_k^e}{D(E_f)} \tag{13}$$

where:-

E_f : Is the Fermi level of the metal ,

$D(E_f)$: Is the density of electronic state at the Fermi level.

This method provides a fast way to calculate the surface charges on the electrodes. As will be shown below, it works perfectly well at equilibrium. However, in out-of-equilibrium simulations, a problem appears on the side of the anode where the metal is dissolved. Since the mobility rapidly decreases with the metal concentration, electrons present on the metallic site before dissolution may be trapped in the electrolyte, leading to spurious electronic charges in the bulk. This problem has been solved in a phenomenological way by adding a term, which relaxes the electronic charge to zero in the electrolyte, to the evolution equation for the electrons[Marc, 2003] ,

$$\frac{\partial P_k^e}{\partial t} = -\sum_a \tilde{J}_{k,k+a}^e - w^e [1 - f_r(P_k^o)] P_k^e \quad (14)$$

where $f_r(p^o)$ is the same interpolation function as f , but with different parameters ξ_r and P_{cr} . With a convenient choice of these parameters, ‘‘electron relaxation’’ occurs only in the liquid.

2.4. Electron transfer

When electron transfer takes places on the electrode surfaces. Metallic cations M^+ located in the electrolyte may receive an electron from a neighboring metallic site and be reduced; in turn, metal atoms in contact with the electrolyte may reject an electron to a neighboring metallic site and become an ion,



The direction of the transfer depends on the relative magnitude of the electrochemical potentials of the involved species. Reduction of cations on a site k of the cathode appears when:

$$\tilde{\mu}_k^+ + \tilde{\mu}_{k+a}^e > \tilde{\mu}_k^o \quad (16)$$

otherwise, the metal is oxidized. Consequently, $\sigma_{k,k+a}$ is defined as the current of electronic charges from $k+a$ to k (current of positive charges from k to $k+a$) reducing the cations on site k (electronic current issued from the oxidation of the metal) via a corresponding elimination (creation) of the electrons on site $k+a$, it is possible to write the reaction rate [Schmickler,1995] ,

$$\sigma_{k,k+a} = \omega_{k,k+a}^* \left(\exp \frac{\tilde{\mu}_k^+ + \tilde{\mu}_{k+a}^e}{KT} - \exp \frac{\tilde{\mu}_k^o}{KT} \right) \quad (17)$$

where:-

$\omega_{k,k+a}^*$: Prefactor of the reaction rate .

This corresponds to an activated electronic charge transfer between the metal surface and the nearest-neighboring cation. The total reduction rate on site k is the sum of all the reaction paths $\sum_a \sigma_{k,k+a}$.

The coefficient $\omega_{k,k+a}^*$ determined from[Bernard,2002] [Marc, 2003]

$$\omega_{k,k+a}^* = \omega^* [1 - f(p_k^o)] f(p_{k+a}^o) \quad (18)$$

where ω^* is a constant frequency factor .In this way , the transfer is localized around the metal-electrolyte interface . The same interpolation $f(p)$ is used for the electron mobility.

3.COMPUTER PROGRAM :-

A program is constructed in visual basic language for one-dimensional system .Through which the determination of concentration at each time and plotting the relationship between concentration (metal, cation, anion, solvent, vacancy) and position are performed which represent growth (in cathode electrode) and dissolution (in anode electrode) show figure (3) .

Equations (3) through (18) are integrated in time by a simple Euler Scheme (constant or variable time step) with dimensionless values .

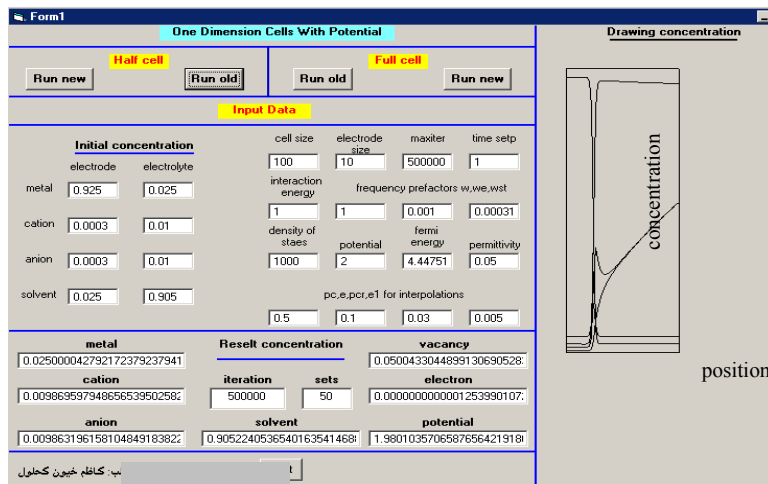


Fig.3. Shows the flow chart of the main program of half and full cell with potential

4.RESULTS AND DISCUSSION :-

When a potential difference (dv) of $2KT/e$ is applied across the cell of size 100 sites contains two identical electrodes of the same thickness of 10 layers . The ionic species start to migrate , a double layer appears on the interface , a reduction process take place at the cathode and the oxidation process take place on the anode . These processes are accelerated by the electric field that can achieved the ions kinetics .

Figures (4 – 9) represents simulation of the different species , namely : (metal , cation , anion , solvent and vacancy) across the sites 50 for the half cell and 100 sites for the full cell with initial ion concentration of 0.01 during the three times intervals $t = (1,3,5) \times 10^5$.

Figures (10 – 12) show the growth of the cathode and the dissolution of the anode . It is noted that the shape of the metal concentration profile across the interface is essentially preserved from the overall configuration view point but with different values.

The interesting results concern the kinetics of the ions . Figures (13 –16) show the evolution of the ion concentration, it is observed that the progressive formation of a concentration gradient between the anode and the cathode with , for cations , a concentration peak on the cathode (accompanied by an electronic layer on the metal surface) . The anion concentration profile presents on the contrary an increase close to the anode . Figure (17) show the total charge distribution at three successive times $t = (1,3,5) \times 10^5$, in addition to the double-layers located around the interfaces, an excess of cations over the anions, on a range of about 30 lattice distances. This extended space charge leads to an important potential drop on the cathode side, as can be seen in figures (18) and (19) that show the electric potential , this is matched with [Bernard ,2001][Marc,2003]

5. CONCLUSIONS :-

Based on the results of this investigation , the following conclusions can be drawn :-

1. The mean-field kinetic equations (MFKE) that are able to reproduce qualitatively the behavior of electrochemical cells with planar electrodes.
2. The growth starts in the one - dimensional electrochemical cells and continues up it maximum value and then gradually stops at time 10^6 for the cell of size (100×10) , while in the cells subjected to potential difference of $2KT/e$, the deposition process continues for a longer time up to anode collapsing .
3. The evolution of the ion concentration is seen to be constant and unchanged in the absence of the potential difference and gradually drops until it stops at time 10^6 , while it has certain gradients under potential difference between the cathode and anode electrodes , furthermore the cation has a peak at the cathode is higher than that of anion concentration and the revers occurs at the anode electrode .

REFERENCES :-

Aogaki R. and Makino T. ,1981," Early Stages of Ramified Growth in Quasi-Two-Dimensional Electrochemical Deposition ", *Electrochim. Acta* , 26 , 1509 .

- Barton J.L. and Bockris J.O'M. ,1962, " Structural Changes Dendrite Deposits During Galvanostatic Electrolysis:A calculation " , Proc.R.Soc.London, Ser.A.268,485.
- Bernard M.-O. , Plapp M. and Gouyet J.-F. , 2001 , " A lattice Gas Model of Electrochemical Cells " , Physica A (to be published) .
- Bernard M.-O. , Plapp M. and Gouyet J.-F. ,2002," A lattice Gas Model of Electrochemical Cells : Mean-Field Kinetic Approach " , Fractal .
- Chen C.and Jorne J.,1990,"Morphological Instability During Electrodeposition", J.Electrochem.Soc.,137,2047.
- Chazalviel J.-N. ,1990," Coulomb Screening by Mobile Charges " , Phys. Rev. A 42, 7355.
- Chen L.Q. ,1994, " Phase - Field Models for Microstructure Evolution " , Acta Metall.Mater.,47,3503 .
- Charles Monroe , and John Newman , 2004, " The Effect of Interfacial Deformation on Electrodeposition Kinetics " , J. Electrochem. Soc. , A880-A886.
- Candacek C. , Riccardo R. , Seung S.H. , Robert A . and Huggins Y . C.,2009," Structural and electrodeposition study of the reaction of lithium with silicon nanowires", J. Power Sources 11523 , No. 6 .
- Diggle J . W. , Despic A.R . and Bokris J.O'M. ,1969,"Experimental Evidence for Homoclinic Chaos in an Electrochemical Growth Process " , J. Electrochem . Sec. , 116 , 503(1969).
- Dobretsov V.Y.,Vaks V.G. and Martin G. ,1996," Coupled Relaxation of Concentration and Order Fields in the Linear Regime " , phys.Rev.B ,54, 3227.
- Gouyet J.-F., Plapp M., Dieterich W. and Maass P. ,2003," Description of Far- From – Equilibrium Processes by Mean- Field Lattice Gas Models " , Adv.Phys.,Vol.52,No.6,PP(523-638) .
- Mullins W.W. and Sekerka R.F.,1963," Morphological Stability of a Particle Growing by Diffusion or Heat Flow", J.Appl.Phys.,34,323 .
- Mathis Plapp and Jean – Francois Gouyet ,1999," Spinodal Decomposition of an ABv model alloy : Patterns at Unstable Surfaces " , Eur. Phys. J. B9 , 267 .
- Marc-Olivier Bernard, Mathis Plapp and Jean-Francois Gouyet,2003,"mean-Field Kinetic lattice Gas Model of Electrochemical Cells " , Phys.Rev.E68,011604 .
- Paolini F., Cabral E.L. and Santos A.,2009," Mean field correction for ions in kinetic equations", IPEN - Inst. de Pesquisas Energeticas e Nucl., Sao Paulo, Brazil .
- Jean – Francois Gouyet and Mathis Plapp , 1996," Interface Dynamics in Mean Field Lattice Gas Model " , Northeastern University Press , 1996.
- Schmickler W. and Henderson D , 1995, " New Models for the Electrochemical Interface,Progress in Surface Science " , Vol. 22, No. 4,PP(323-420).
- Vincent C.A. and Scrosati B. ,1997," Modern Batteries " , Publishers , London ; see also the web site, <<http://www.corrosion-doctors.org> for general information on Batteries, corrosion, and electrodeposition.

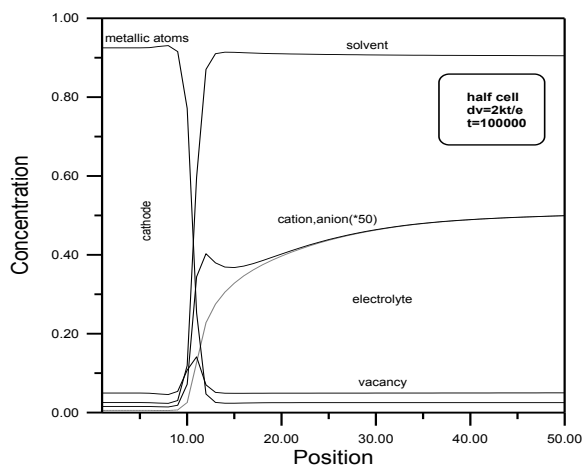


Fig.4. Concentration profiles across a 50-site cell.

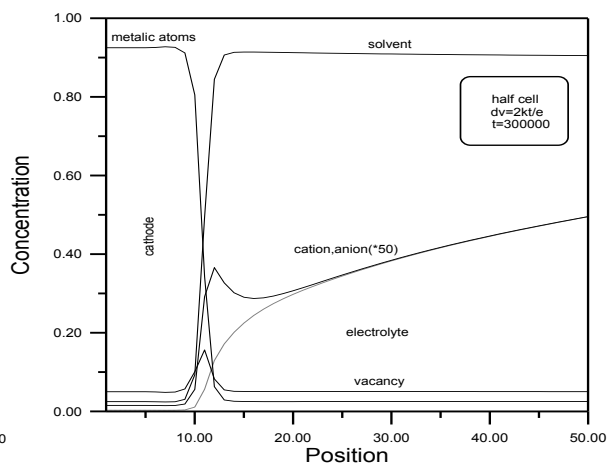


Fig.5. Concentration profiles across a 50-site cell.

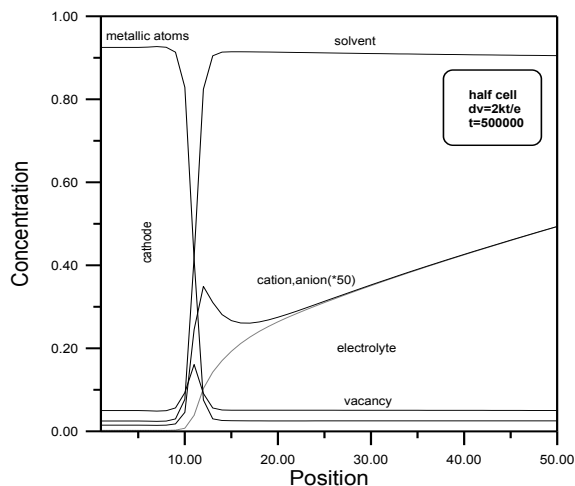


Fig.6. Concentration profiles across a 50-site cell.

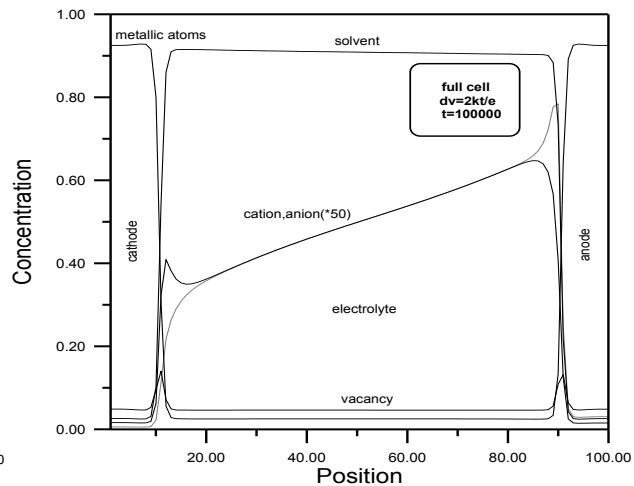


Fig.7. Concentration profiles across a 100-site cell.

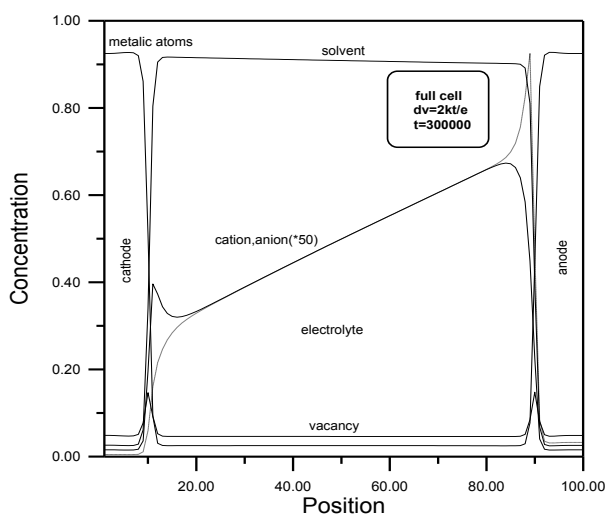


Fig.8. Concentration profiles across a 100-site cell.

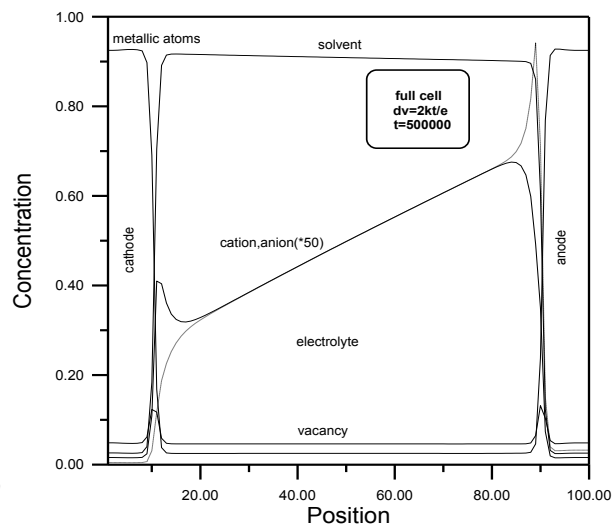


Fig.9. Concentration profiles across a 100-site cell.

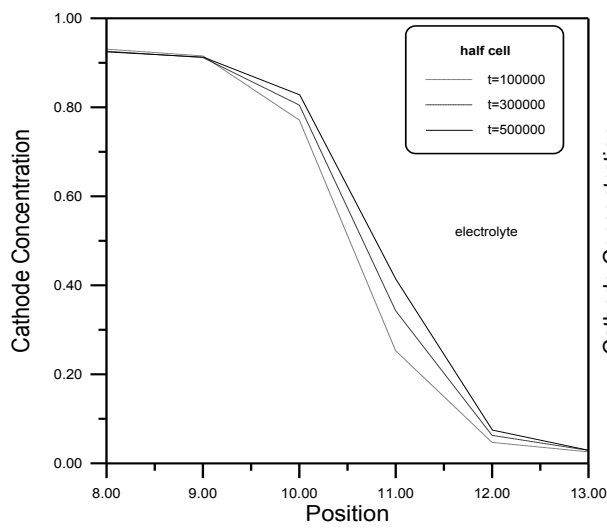


Fig.10. Showing the electrode position (reduction) at the cathode.

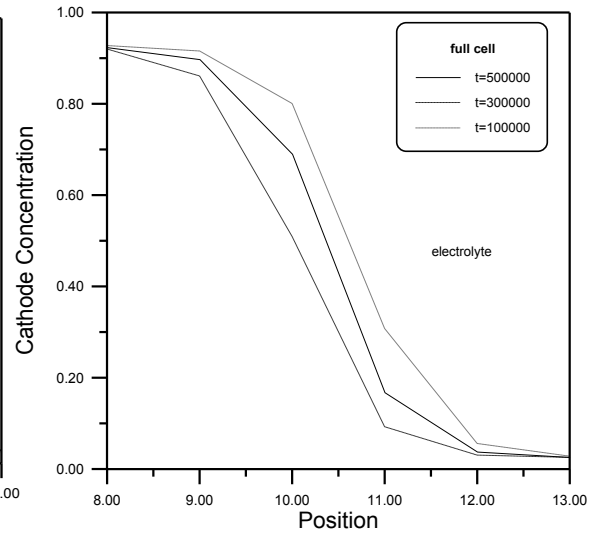


Fig.11. Showing the electrode position (reduction) at the cathode.

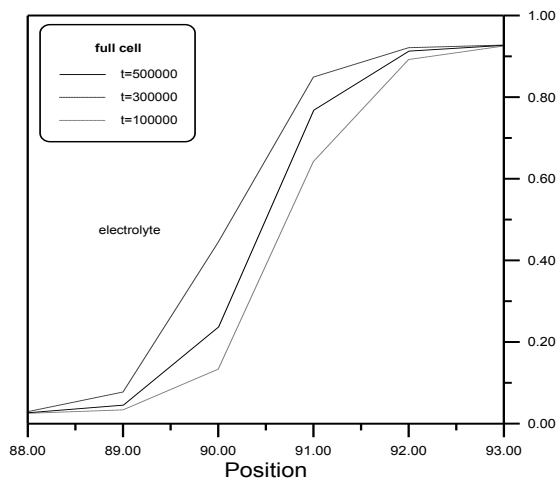


Fig.12. Showing the dissolution of metal at the anode

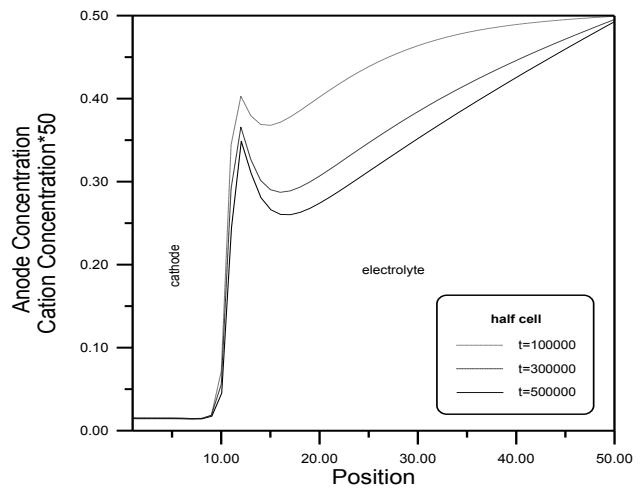


Fig.13. Cation concentration profiles.

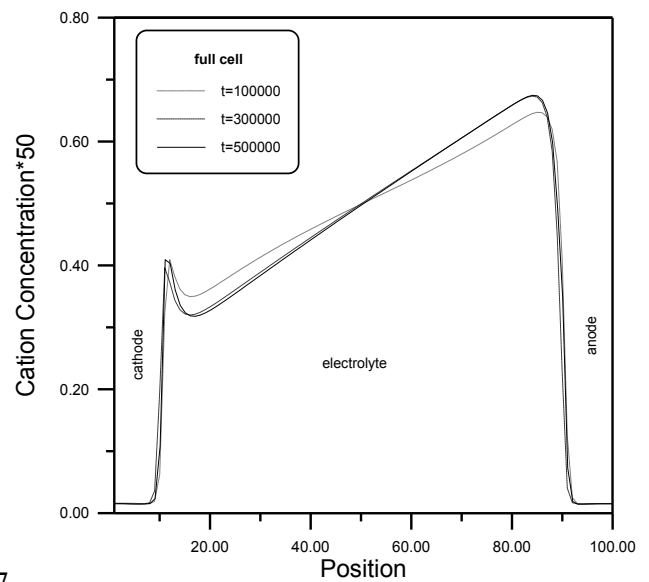
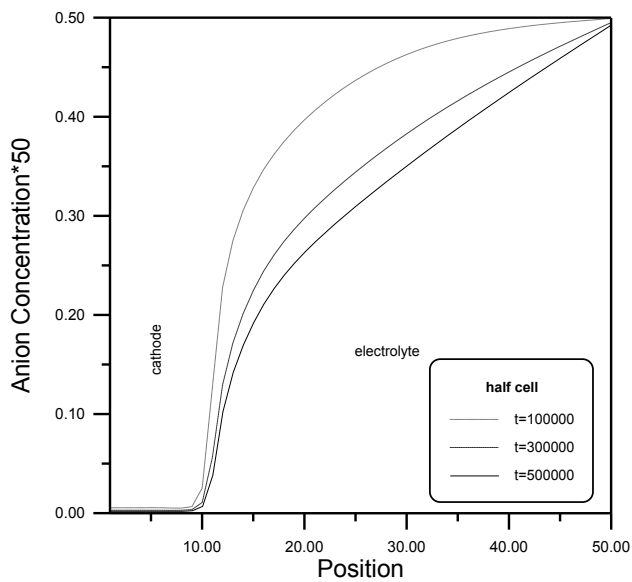


Fig.14. Anion concentration profiles

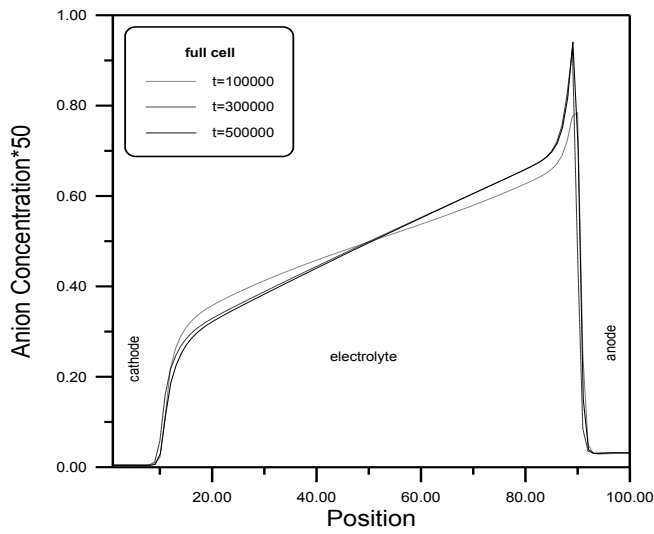


Fig.15. Cation concentration profiles

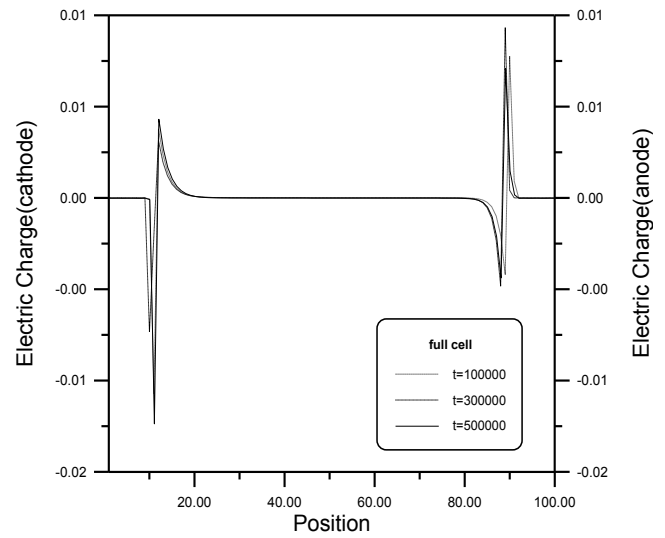


Fig.16. Anion concentration profiles

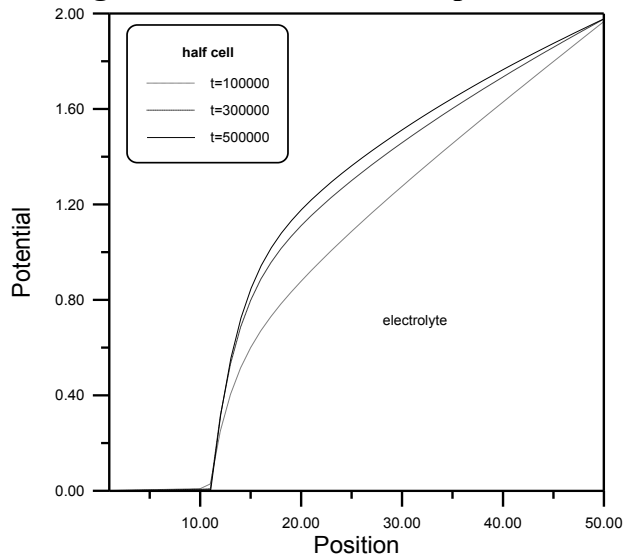


Fig.18. Potential profiles

Fig.17. Charge distribution.

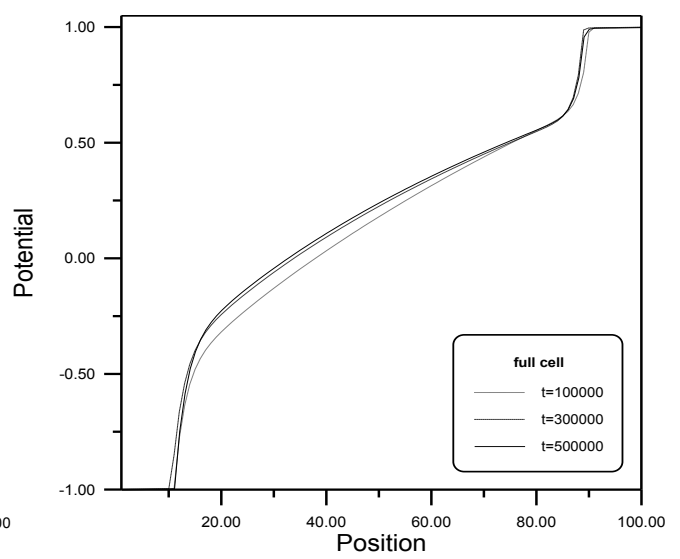


Fig.19. Potential profiles